HHS Public Access

Author manuscript

Chemistry. Author manuscript; available in PMC 2018 January 23.

Published in final edited form as:

Chemistry. 2017 January 23; 23(5): 1145–1150. doi:10.1002/chem.201604842.

Aqueous Eu^{II} Oxidation Rate Tuned by Coordination Environment

Dr. Levi A. Ekanger, **Lina A. Basal**, and **Prof. Matthew J. Allen***

Department of Chemistry, Wayne State University, 5101 Cass Avenue, Detroit, MI 48202 (USA)

Abstract

The $Eu^{II/III}$ redox couple offers metal-based oxidation-sensing with magnetic resonance imaging making the study of Eu^{II} oxidation chemistry important in the design of new probes. Accordingly, we explored oxidation reactions with a set of Eu^{II}-containing complexes. We report the observation of superoxide formation from the reaction between Eu^{II} and dioxygen using electron paramagnetic resonance spectroscopy. Additionally, we report oxidation kinetics of three Eu^{II}-containing complexes with bromate and glutathione disulfide at pH values including 5 and 7. In the reaction with bromate, the oxidation rate of two of the complexes increased by 7.3 and 6.7× upon decreasing pH from 7 to 5, but the rate increased by 17× for a complex containing amide functional groups over the same pH range. The oxidation rate of a fluorobenzo-functionalized cryptate was relatively slow, indicating that the ligand used to impart thermodynamic oxidative stability might also be useful for controlling oxidation kinetics.

Graphical abstract

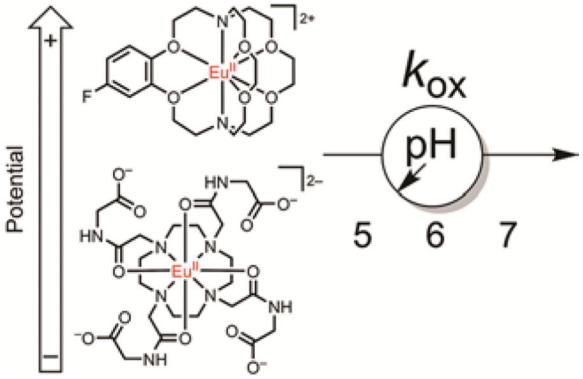

Release the electron: The oxidation chemistry of Eu^{II}-containing cyclen-, aqua-, and cryptand-based complexes was explored. The oxidation of Eu^{II} by BrO_3^- was faster at pH 5 than pH 7 for all complexes, but the oxidation rate of the cyclen-based tetraglycinate complex was relatively sensitive to changes in pH. A general lack of reactivity between Eu^{II} and glutathione disulfide was suggestive of activation barriers to the reaction over a 4 h period.

* mallen@chem.wayne.edu, Homepage: http://chem.wayne.edu/allengroup.

Supporting information for this article is given via a link at the end of the document.

Keywords

chelates; imaging agents; kinetics; lanthanides; redox chemistry

Introduction

The redox chemistry of lanthanides has received increasing attention over recent years because their +2, +3, and +4 oxidation states show promise for applications such as single-molecule and single-ion magnetism,[1] luminescence,[2] stoichiometric and catalytic reductions,[3] and redox-responsive magnetic resonance imaging (MRI).[4–7] Out of the lanthanide ions, Eu^{II} is uniquely poised for oxidation-responsive MRI because (1) some Eu^{II}-containing complexes are stable in aqueous media, (2) Eu^{II} provides positive (bright or T_1-shortening) contrast enhancement in MRI, (3) the $E_{1/2}$ of $Eu^{II/III}$ can be tuned over a physiologically relevant range, and (4) the +2 and +3 oxidation states of Eu exhibit different magnetic and spectroscopic characteristics making responsive imaging feasible.[7,8] The oxidation-responsive behavior of Eu^{II}-containing complexes has been documented in vivo,[5,6] making the kinetics of oxidation under physiological conditions important to understand for the rational design of new complexes. Accordingly, there is a need for kinetic and thermodynamic analyses to enable a detailed understanding of Eu^{II}-containing complexes for responsive MRI. Here, we report that superoxide (O_2^-) is a product of the reaction between O_2 and $EuCl_2$ using a radical trap and electron paramagnetic resonance (EPR) spectroscopy. We also report the rates of oxidation of three Eu^{II}-containing complexes in the presence of bromate (BrO_3^-) and glutathione disulfide (GSSG) in aqueous media at pH 5 and 7.

Aqueous Eu^{II} oxidation chemistry for electron-transfer reactions has been explored within the context of Marcus theory for self-exchange redox reactions,[9–11] where the europium self-exchange ($Eu^{II}_a + Eu^{III}_b \rightarrow Eu^{III}_a + Eu^{II}_b$) reaction rate ($k \leq 3 \times 10^{-5}$ M^{-1} s^{-1}) is slower than the corresponding $Fe^{II/III}$ self-exchange reaction rate ($k = 4$ M^{-1} s^{-1}).[10] One explanation for the discrepancy in self-exchange reaction rates involves the radial constriction of 4f orbitals relative to 3d orbitals.[10] A separate explanation invokes different energetic barriers for Eu and Fe self-exchange reactions imposed by solvent reorganizational energy.[10] Regardless of the differences between $Eu^{II/III}$ and $Fe^{II/III}$ self-exchange chemistry, the non-self-exchange oxidation of Eu^{II} is an important reaction to study because it can be used to help understand the behavior of Eu^{II} under physiological conditions. Non-self-exchange Eu^{II} electron-transfer has been explored using the Eu^{II} aqua ion in strongly acidic media.[12] Also in acidic media, the rate of oxidation of the Eu^{II} aqua ion by hydrogen peroxide was slowed by chelation of Eu^{II} with cyclic crown ethers and cryptands.[13] Studying the oxidation chemistry of chelated Eu^{II} under conditions representative of physiological conditions would be more relevant to redox-responsive MRI. We sought to build upon the observations in acidic solution by exploring the oxidation of Eu^{II}-containing complexes in buffered aqueous media. Before performing kinetic measurements, we studied a fundamental reaction between $EuCl_2$ and O_2 to determine if an oxygen-containing product could be identified. Given the in vivo correlation between tissue pO_2 and the persistence of

Eu^{II}-based positive contrast enhancement,[5,6] these studies are important for rationalizing Eu^{II} oxidation-responses.

Results and Discussion

Eu^{II} is a one-electron reductant, and a one-electron reduction of O_2 produces O_2^-. To gain insight into the oxidation of Eu^{II} by O_2, we used the EPR spin trap 5-*tert*-butoxycarbonyl 5-methyl-1-pyrroline *N*-oxide (BMPO). BMPO is capable of reacting with O_2^- to form a relatively stable radical adduct that is observable with EPR spectroscopy.[14] To better our chances of observing a radical product, we used methanol as the solvent because O_2^- is more stable in non-aqueous than aqueous media.[15] Because we did not measure reaction kinetics, the use of physiological conditions was not necessary to identify a reaction product from $EuCl_2$ exposed to O_2. A direct reaction between $EuCl_2$ and BMPO was not observed, but a radical signal was observed upon bubbling O_2 into a solution containing $EuCl_2$ and BMPO (Figure 1). When KO_2 was added as a source of O_2^- to BMPO, an EPR profile nearly identical to the product of $EuCl_2$ reacting with O_2 was observed (Figure 1). However, the EPR spectrum of KO_2 in the absence of BMPO did not produce the same EPR signal. The relatively small line shape differences between the EPR spectra of O_2 reacting with $EuCl_2$ in the presence of BMPO and KO_2 in the presence of BMPO (Figure 1B) can be explained by the presence of Eu^{III} ions in the former sample. Eu^{III} has a diamagnetic ground state ($^7F_0$) and thermally accessible excited states, such as $^7F_1$, that have nonzero effective magnetic moments. Population of the $^7F_1$ excited state has been observed at 8 K,[16] and it is therefore reasonable that a paramagnetic excited state was populated to some extent at 110 K. Additionally, it could be envisioned that the hydroperoxyl–BMPO radical adduct coordinated to Eu^{III}, and this interaction caused a relatively small perturbation in the chemical environment of the unpaired electron of the hydroperoxyl–BMPO radical adduct. When KO_2 was mixed with BMPO in the presence of $EuCl_3$ as a direct source of Eu^{III}, a similar line shape difference was observed as from the reaction between $EuCl_2$, O_2, and BMPO (Figure S1). This experiment indicates that the line shape differences are due to the presence of Eu^{III}. Regardless of the small differences between the spectra in Figure 1, these data suggest that O_2^- is a product of the reaction between O_2 and $EuCl_2$. After demonstrating the formation of O_2^-, we turned our attention to aqueous oxidation reactions for kinetic and thermodynamic analyses.

We measured the kinetics of oxidation of Eu^{II}-containing complexes **1**-Eu^{II}, $EuCl_2$(aq), and **2**-Eu^{II} (Figure 2) because $EuCl_2$(aq) is an aqueous analogue of $EuCl_2$ used in our EPR studies, and **1**-Eu^{II} and **2**-Eu^{II} have been used for oxidation-responsive imaging.[5,6] Additionally, **1**-Eu^{II}, $EuCl_2$(aq), and **2**-Eu^{II} encompass a relatively wide range in reduction potentials (Table 1) with **1**-Eu^{II} being 374 mV more negative than $EuCl_2$(aq)[7] and **2**-Eu^{II} being 547 mV more positive than $EuCl_2$(aq).[17] Although we have observed rapid oxidation of Eu^{II} by gaseous diatomic molecules, such as O_2 and NO, we elected to study reaction kinetics with non-gaseous oxidants for the ease of quantifying and handling in an inert atmosphere. Because of our in vivo observations between pO_2 and Eu^{II} oxidation and the EPR data with O_2 presented in this work, we chose the anion BrO_3^- as a substitute for O_2 for kinetic measurements. While structurally different, the relatively positive reduction potentials of BrO_3^- and O_2 (1.06 and 0.815 mV vs normal hydrogen electrode,[18–20]

respectively, at pH 7) indicate that BrO_3^- should, from a thermodynamic standpoint, spontaneously oxidize **1**-Eu^{II}, $EuCl_2$(aq), and **2**-Eu^{II}. It should be noted that similarly positive reduction potentials do not equate to similar oxidation rates. GSSG was chosen as an oxidant because it is a major component of the cellular redox buffer along with reduced glutathione.[20] GSSG was expected to react spontaneously with **1**-Eu^{II} and $EuCl_2$(aq) but not react with **2**-Eu^{II} based on Gibbs free energies calculated using electrochemical data (Table 1). We expected that a wide range in Eu^{II} reductant strength and ligand structure combined with relatively strong-to-intermediate oxidants would yield fundamental information regarding aqueous oxidation chemistry of Eu^{II}-containing complexes via comparison of reaction rates in aqueous media.

To measure the kinetics of oxidation of **1**-Eu^{II}, $EuCl_2$(aq), and **2**-Eu^{II} by BrO_3^- and GSSG, loss of Eu^{II} was monitored using normalized UV–visible absorbance as a function of time (Figure 3). Experiments were conducted at pH 5, 6, and 7 because these values encompass a physiologically relevant range of pH values.[21] A reaction time of 240 min was chosen because it is longer than the clearance half-life (18 min) of small lanthanide-containing complexes from rats,[22] and therefore, represents a relevant period of time to observe oxidation events. Absorbance was measured at the maximum value for each complex: 353 nm for **1**-Eu^{II} and 320 nm for $EuCl_2$(aq) and **2**-Eu^{II} (see Figure S2 for representative spectra). The absorption of UV–visible light at wavelengths longer than 300 nm was not observed for the Eu^{III}-containing reaction products, indicating that decreases in absorbance are the result of oxidation of Eu^{II}. Oxidation rate (k_{ox}) data (Table 2) revealed the acceleration of Eu^{II} oxidation upon lowering the pH from 7 to 5 for every reaction with BrO_3^-, but oxidation was not observed for any Eu^{II}-containing complex at either pH with GSSG. Reactions with GSSG at pH 6 were not performed because no reactivity was observed at pH 5 or 7. There were increases of 1.4 and 2.3× in k_{ox} from pH 7 to 6 for $EuCl_2$(aq) and **2**-Eu^{II}, respectively, in the reaction with BrO_3^-. The same reactions with BrO_3^- resulted in increases in k_{ox} of 5.3 and 2.9× from pH 6 to 5 for $EuCl_2$(aq) and **2**-Eu^{II}, respectively. However, there was no increase in k_{ox} from pH 7 to 6 and a 17× increase in k_{ox} from pH 6 to 5 for the reaction of **1**-Eu^{II} with BrO_3^-. The relatively large increase in k_{ox} for **1**-Eu^{II} upon decreasing from pH 6 to 5 caused a change in the order of oxidation rates of the three Eu-containing species from $EuCl_2$(aq) > **1**-Eu^{II} > **2**-Eu^{II} at pH 7 and 6 to **1**-Eu^{II} > $EuCl_2$(aq) > **2**-Eu^{II} at pH 5. The 17× increase in k_{ox} and the switch in order of oxidation rates demonstrate that **1**-Eu^{II} had a relatively high sensitivity to change in solution pH.

The relatively high sensitivity of k_{ox} to pH for **1**-Eu^{II} can be explained by protons associated with **1**-Eu^{II}. The exchange rate of amide protons on the macrocyclic tetraglycinate ligand of **1**-Eu^{II} with trivalent lanthanides is pH-dependent.[23] The exchange rate of amide protons on **1**-Eu^{III} has been examined using radiofrequency saturation transfer of amide protons to bulk water protons at pH 5 (extremely slow amide-proton exchange, $k_{ex} < 127\ s^{-1}$) and pH 7 ($k_{ex} = 127\ s^{-1}$).[24] Therefore, it could be envisioned that hydrogen bonding between amide protons on **1**-Eu^{II} and oxygen atoms on BrO_3^- persist to a greater extent at pH 5 than at pH 6 or 7. The water exchange rate of **1**-Eu^{III} ($k_{ex} = 5.8 \times 10^4\ s^{-1}$)[24] is orders of magnitude faster than amide proton exchange and is insensitive to changes in pH from 5–8.[23,24] Labile water molecules on $EuCl_2$(aq) and the absence of exchangeable protons on the macrocyclic

ligand of **2**-Eu^{II} likely preclude these complexes from participating in comparable hydrogen bonding interactions with BrO_3^-. The water-exchange rate of $EuCl_2$(aq) ($k_{ex} = 4.4 \times 10^9$ s^{-1})[25] and a structurally analogous complex to **2**-Eu^{II} ($k_{ex} = 8.5 \times 10^7$ s^{-1})[26] indicate that coordinated water molecules are too fleeting to participate in a similar hydrogen bonding interaction as expected for amide protons. Coordinated water molecules on $EuCl_2$(aq) and **2**-Eu^{II} might contribute to the observed change in k_{ox}, but the relatively large change in k_{ox} for **1**-Eu^{II} is likely due to proton exchange occurring on the macrocyclic ligand rather than labile monodentate water molecules. Accordingly, the relatively slow exchange of amide protons on **1**-Eu^{II} at pH 5 could allow these protons to hydrogen bond with BrO_3^- in the vicinity of Eu^{II}, thereby increasing the probability of electron transfer. Upon neutralization to pH 7, the hydrogen-bonding interactions are interrupted by relatively fast exchange of amide protons on **1**-Eu^{II}, thereby decreasing the probability of electron transfer. Protonation of a carboxylate group on **1**-Eu^{II} could also explain the relatively large increase in k_{ox} at pH 5. Protonation would lower the overall charge of the complex and could result in a hydrogen-bonding interaction with BrO_3^-. Protonation studies of similar tetraglycinate complexes have been reported.[27]

The order of oxidation rates $EuCl_2$(aq) > **2**-Eu^{II} was observed at pH 7, 6, and 5. This observation can be explained by the cryptand of **2**-Eu^{II} inhibiting access to the metal center by decreasing available coordination sites from 9 or 10 in $EuCl_2$(aq) to 1 or 2 in **2**-Eu^{II}.[5] A similar explanation was used to rationalize the decreased rate of Eu^{II} oxidation by hydrogen peroxide upon chelation in crown ethers and cryptands.[13] In that study, the decreased oxidation rate was attributed to the steric protection of Eu^{II} ions within appropriately sized ligands. By the same logic, $EuCl_2$(aq) would be expected to have more available coordination sites than **1**-Eu^{II}, indicating that the order of oxidation rates should be $EuCl_2$(aq) > **1**-Eu^{II} at pH 7, 6, and 5. $EuCl_2$(aq) was oxidized the fastest at pH 7 and 6, but the order of oxidation rates switched to **1**-Eu^{II} > $EuCl_2$(aq) at pH 5. Therefore, the ability of BrO_3^- to access open coordination sites on Eu^{II} cannot explain these data without another factor governing oxidation rate. A likely factor is the hydrogen-bonding interaction between **1**-Eu^{II} and BrO_3^- described above.

Unlike BrO_3^-, GSSG did not react with **1**-Eu^{II}, $EuCl_2$(aq), or **2**-Eu^{II} during the course of the 240 min experiment at pH 5 or 7. The negative Gibbs free energies of electron transfer between GSSG and **1**-Eu^{II} or $EuCl_2$(aq) indicate that spontaneous reactions should occur between GSSG and these two complexes. The lack of reactivity observed in our experiments indicates the presence of an activation barrier, possibly from the inability of the disulfide bond to access the Eu^{II} metal center, preventing disulfide reduction over a 240 min period. Unlike **1**-Eu^{II} and $EuCl_2$(aq), the lack of reactivity between **2**-Eu^{II} and GSSG can be explained by positive Gibbs free energies at pH 5 and 7 (Table 1), indicating that spontaneous reactions should not be observed. Altogether, the GSSG data and in vivo imaging experiments[5,6] indicate that, from a biological standpoint, bulky disulfide bonds or other bulky oxidizing agents are likely minor contributors at most to Eu^{II} oxidation in vivo for imaging experiments shorter than four hours.

Conclusions

Our findings provide insight into the oxidation chemistry of Eu^{II}-containing complexes, such as the formation of O_2^-, the role of the ligand in Eu^{II} oxidation rate, and reaction barriers with disulfide bonds. We expect that the ability to rationally design Eu^{II}-containing complexes to tune both thermodynamic stability and kinetics of oxidation will be invaluable in the design of new oxidation-responsive complexes for MRI.

Experimental Section

General remarks

Commercially available chemicals were of reagent-grade purity or better and were used without further purification unless otherwise noted. The EPR spin trap BMPO was purchased from Applied Bioanalytical Labs. Water was purified using a PURELAB Ultra Mk2 water purification system (ELGA). Water and methanol were degassed under reduced pressure prior to use. Oxidation rates were obtained from the slope of natural logarithm of absorbance as a function of time.

Inductively coupled plasma mass spectrometry (ICP–MS)

Measurements of Eu concentrations were acquired on an Agilent Technologies 7700 series ICP–MS instrument at the Lumigen Instrument Center in the Department of Chemistry at Wayne State University. All dilutions were performed with aqueous 2% HNO_3, which was also used for blank samples during calibration. Calibration curves were created using the ^{153}Eu isotope ion count for a 1–200 ppb concentration range (diluted from Fluka ICP standard solution, Eu_2O_3 in aqueous 2% HNO_3, 1000 mg Eu/L). All samples were diluted to fall within this range.

EPR spectroscopy

EPR spectroscopy was performed with a Bruker EMX X-band spectrometer equipped with an Oxford variable-temperature cryostat. Acquisition parameters included a temperature of 110 K, microwave frequency of 9.3696 GHz, microwave power of 1.99 mW, modulation amplitude of 1.0 G (with 10 points per modulation amplitude). EPR samples were prepared under an inert atmosphere of Ar within a glovebox, were a total volume of 0.3 mL, and were sealed with wax under an atmosphere of Ar in Norell SEPR250S EPR tubes. Solutions were prepared by dissolving $EuCl_2$ (1.7 mg, 7.6 μmol) and BMPO (1.1 mg, 5.0 μmol) in methanol (0.450 mL). After measuring the sample under an Ar atmosphere, O_2 was bubbled directly into the sample solution within the EPR tube for 15 s. The sample was measured 5 min after bubbling O_2. The positive control with KO_2 was prepared by adding a methanolic solution (0.5 mL) containing BMPO (12 mM) to solid KO_2 (0.4 mg, 6 μmol). The control with a direct source of Eu^{III} was prepared in the same manner as the positive control with KO_2, but with the addition of $EuCl_3{\cdot}6H_2O$ (2.8 mg, 7.6 μmol). The resulting mixtures were stirred vigorously for 15 s before filtering through a 0.2 μm hydrophilic filter into EPR tubes. The resulting samples were measured 5 min after exposure to KO_2. The same procedure was used for the sample containing KO_2 without BMPO.

Preparation of buffer and oxidant solutions for UV–visible spectroscopy

Buffer for pH 5 reactions was prepared by dissolving sodium acetate trihydrate (68.0 mg, 0.500 mmol) in water (9.00 mL). The solution pH was adjusted to 5 with the addition of aqueous HCl (0.1 M). Additional water was used to obtain a final volume of 10.0 mL. Buffer for pH 6 reactions was prepared by dissolving 2-morpholinoethane-1-sulfonic acid (211.4 mg, 1.083 mmol) in water (10.0 mL). The solution pH was adjusted to 6 with the addition of aqueous NaOH (0.1 M). Additional water was used to obtain a final volume of 20.0 mL. Buffer for pH 7 reactions was prepared by dissolving 3-morpholinopropane-1-sulfonic acid (104.6 mg, 0.500 mmol) in water (9.00 mL). The solution pH was adjusted to 7 with the addition of aqueous NaOH (0.1 M). Additional water was added to obtain a final volume of 10.0 mL. An aqueous stock solution of BrO_3^- was prepared by dissolving potassium bromate (83.5 mg, 0.500 mmol) in water (4.50 mL). The pH was either left neutral for pH 7 reactions or adjusted to pH 5 or 6 with the addition of aqueous HCl (0.1 M). Additional water was used to reach a final volume of 5.00 mL. An aqueous stock solution of GSSG was prepared by dissolving L-glutathione oxidized (306.3 mg, 0.500 mmol) in water (4.50 mL). The pH was increased to 5 or 7 with the addition of aqueous NaOH (0.1 M). Additional water was used to obtain a final volume of 5.00 mL.

Preparation of tetraglycinate complex for UV–visible spectroscopy (1-Eu^{II})

The preparation of **1**-Eu^{II} was adapted from a reported procedure.[7] Briefly, **1**-Eu^{III}·$9H_2O$ (2.00 mg, 2.12 μmol, Macrocyclics) was reduced with Zn dust (30 mg, 0.46 mmol) in water (1.00 mL) followed by filtration through a 0.2 μm hydrophilic filter. DOWEX cation-exchange resin was used to exchange Zn^{2+} with Na^+, and resin was removed by filtration through a 0.2 μm hydrophilic filter. To the resulting solution containing **1**-Eu^{II} was added water (400 μL), aqueous buffer (400 μL of a 50.0 mM solution), and aqueous oxidant (200 μL of a 100 mM solution) to yield the final reaction solution [2.00 mL of **1**-Eu^{II} (1.00 mM), buffer (10.0 mM), and oxidant (10.0 mM)].

Preparation of aqua complex for UV–visible spectroscopy ($EuCl_2$(aq))

To water (1303 μL) was added aqueous $EuCl_2$ (97.1 μL of a 20.6 mM solution), aqueous buffer (400 μL of a 50.0 mM solution), and aqueous oxidant (200 μL of a 100 mM solution) to yield the final reaction solution [2.00 mL of $EuCl_2$(aq) (1.00 mM), buffer (10.0 mM), and oxidant (10.0 mM)].

Preparation of 4-fluorobenzo-functionalized complex for UV–visible spectroscopy (2-Eu^{II})

The synthesis and characterization of the 4-fluorobenzo-functionalized ligand is described elsewhere.[5] To water (1259 μL) was added aqueous $EuCl_2$ (97.1 μL of a 20.6 mM solution) and aqueous 4-fluorobenzo-functionalized ligand (44.0 μL of a 50.0 mM solution). The resulting solution was stirred at ambient temperature under an inert atmosphere for 2 h before the addition of aqueous buffer (400 μL of a 50.0 mM solution) and aqueous oxidant (200 μL of a 100 mM solution) to yield the final reaction solution [2.00 mL of **2**-Eu^{II} (1.00 mM), buffer (10.0 mM), and oxidant (10.0 mM)].

UV–visible data acquisition

Studies were performed under an atmosphere of N_2 in a wet glovebox (water allowed, O_2 excluded) using an Ocean Optics STS microspectrometer (STS-UV-L-25-400-SMA) coupled to an Ocean Optics high power DH-MINI deuterium tungsten halogen source with shutter (200–2000 nm). A cuvette holder (CUV-UV) equipped with a cover (CUV-COVER) was used to measure samples within the glovebox over a 4 h period. Optical fibers (solarization-resistant, 400 μm optical fibers 1 m in length) from the light source and spectrometer (outside of the glovebox) were connected to both ends of the cuvette holder (inside the glovebox) using a dual VFT, KF-40 flange adapter (2–450 μm XSR) and with a total of 4 × 1 m of optical fiber. Samples were housed in individual air-tight quartz cuvettes and remained capped between measurements. Caps were removed from cuvettes during the measurements because the cuvette cover used to block ambient light would not accommodate the cap. Final reaction solutions (described above) were prepared within the cuvette and were stirred for 15 s prior to the initial measurement, but were not stirred between subsequent measurements. The integration time used for all measurements was 10,000 ms.

Supplementary Material

Refer to Web version on PubMed Central for supplementary material.

Acknowledgments

This work was supported by the National Institutes of Health (R01EB013663), and L. A. E. is grateful to Wayne State University for a Summer Dissertation Fellowship.

References

1. a) Meihaus KR, Fieser ME, Corbey JF, Evans WJ, Long JR. J. Am. Chem. Soc. 2015; 137:9855–9860. [PubMed: 26168303] b) Blagg RJ, Ungur L, Tuna F, Speak J, Comar P, Collison D, Wernsdorfer W, McInnes EJL, Chibotaru LF, Winpenny REP. Nat. Chem. 2013; 5:673–678. [PubMed: 23881498]
2. a) Kuda-Wedagedara ANW, Wang C, Martin PD, Allen MJ. J. Am. Chem. Soc. 2015; 137:4960–4963. [PubMed: 25853298] b) Kelly RP, Bell TDM, Cox RP, Daniels DP, Deacon GB, Jaroschik F, Junk PC, Le Goff XF, Lemercier G, Martinez A, Wang J, Werner D. Organometallics. 2015; 34:5624–5636.c) de Bettencourt-Dias A, Barber PS, Bauer S. J. Am. Chem. Soc. 2012; 134:6987–6994. [PubMed: 22503109]
3. a) Yin H, Carroll PJ, Anna JM, Schelter EJ. J. Am. Chem. Soc. 2015; 137:9234–9237. [PubMed: 26151154] b) Chciuk TV, Anderson WR Jr, Flowers RA II. Angew. Chem. 2016; 128:6137–6140.Angew. Chem. Int. Ed. 2016; 55:6033–6036.
4. a) Tsitovich PB, Burns PJ, McKay AM, Morrow JR. J. Inorg. Biochem. 2014; 133:143–154. [PubMed: 24529651] b) Ekanger LA, Ali MM, Allen MJ. Chem. Commun. 2014; 50:14835–14838.c) Ratnakar SJ, Soesbe TC, Lumata LL, Do QN, Viswanathan S, Lin C-Y, Sherry AD, Kovacs Z. J. Am. Chem. Soc. 2013; 135:14904–14907. [PubMed: 24050192]
5. Ekanger LA, Polin LA, Shen Y, Haacke EM, Martin PD, Allen MJ. Angew. Chem. 2015; 127:14606–14609.Angew. Chem. Int. Ed. 2015; 54:14398–14401.
6. Ekanger LA, Polin LA, Shen Y, Haacke EM, Allen MJ. Contrast Media Mol. Imaging. 2016; 11:299–303. [PubMed: 27028559]
7. Ekanger LA, Mills DR, Ali MM, Polin LA, Shen Y, Haacke EM, Allen MJ. Inorg. Chem. 2016; 55:9981–9988. [PubMed: 27244124]

8. Ekanger LA, Allen MJ. Metallomics. 2015; 7:405–421. [PubMed: 25579206]
9. Meier DJ, Garner CS. J. Phys. Chem. 1952; 56:853–857.
10. Balzani V, Scandola F, Orlandi G, Sabbatini N, Indelli MT. J. Am. Chem. Soc. 1981; 103:3370–3378.
11. Yee EL, Hupp JT, Weaver MJ. Inorg. Chem. 1983; 22:3465–3470.
12. a) Candlin JP, Halpern J, Trimm DL. J. Am. Chem. Soc. 1964; 86:1019–1022.b) Adin A, Sykes AG. Nature. 1966; 209:804.c) Adin A, Sykes AG. J. Chem. Soc. A. 1966:1230–1236.d) Carlyle DW, Espenson JH. J. Am. Chem. Soc. 1968; 90:2272–2278.e) Chou M, Creutz C, Sutin N. J. Am. Chem. Soc. 1977; 99:5615–5623.f) Muralidharan S, Espenson JH. Inorg. Chem. 1984; 23:636–639.
13. Staninski K, Kaczmarek M, Schroeder G, Elbanowski M. Monatsh. Chem. 1999; 130:1311–1318.
14. Zhao H, Joseph J, Zhang H, Karoui H, Kalyanaraman B. Free Radic. Biol. Med. 2001; 31:599–606. [PubMed: 11522444]
15. Dvoranová D, Barbieriková Z, Brezová V. Molecules. 2014; 19:17279–17304. [PubMed: 25353381]
16. You H, Nogami M. J. Phys. Chem. B. 2004; 108:12003–12008.
17. Gamage N-DH, Mei Y, Garcia J, Allen MJ. Angew. Chem. 2010; 122:9107–9109.Angew. Chem. Int. Ed. 2010; 49:8923–8925.
18. Ding L, Li Q, Cui H, Tang R, Xu H, Xie X, Zhai J. Electrochim. Acta. 2010; 55:8471–8475.
19. Feig AL, Lippard SJ. Chem. Rev. 1994; 94:759–805.
20. Schafer FQ, Buettner GR. Free Radic. Biol. Med. 2001; 30:1191–1212. [PubMed: 11368918]
21. Gerweck LE, Seetharaman K. Cancer Res. 1996; 56:1194–1198. [PubMed: 8640796]
22. Bousquet J-C, Saini S, Stark DD, Hahn PF, Nigam M, Wittenberg J, Ferrucci JT Jr. Radiology. 1988; 166:693–698. [PubMed: 3340763]
23. a) Aime S, Barge A, Castelli DD, Fedeli F, Mortillaro A, Nielsen FU, Terreno E. Magn. Reson. Med. 2002; 47:639–648. [PubMed: 11948724] b) Aime S, Castelli DD, Terreno E. Angew. Chem. 2002; 114:4510–4512.Angew. Chem. Int. Ed. 2002; 41:4334–4336.
24. Terreno E, Castelli DD, Cravotto G, Milone L, Aime S. Invest. Radiol. 2004; 39:235–243. [PubMed: 15021328]
25. Caravan P, Tóth É, Rockenbauer A, Merbach AE. J. Am. Chem. Soc. 1999; 121:10403–10409.
26. Garcia J, Neelavalli J, Haacke EM, Allen MJ. Chem. Commun. 2011; 47:12858–12860.
27. Baranyai Z, Brücher E, Iványi T, Király R, Lázár I, Zékány L. Helv. Chim. Acta. 2005; 88:604–617.

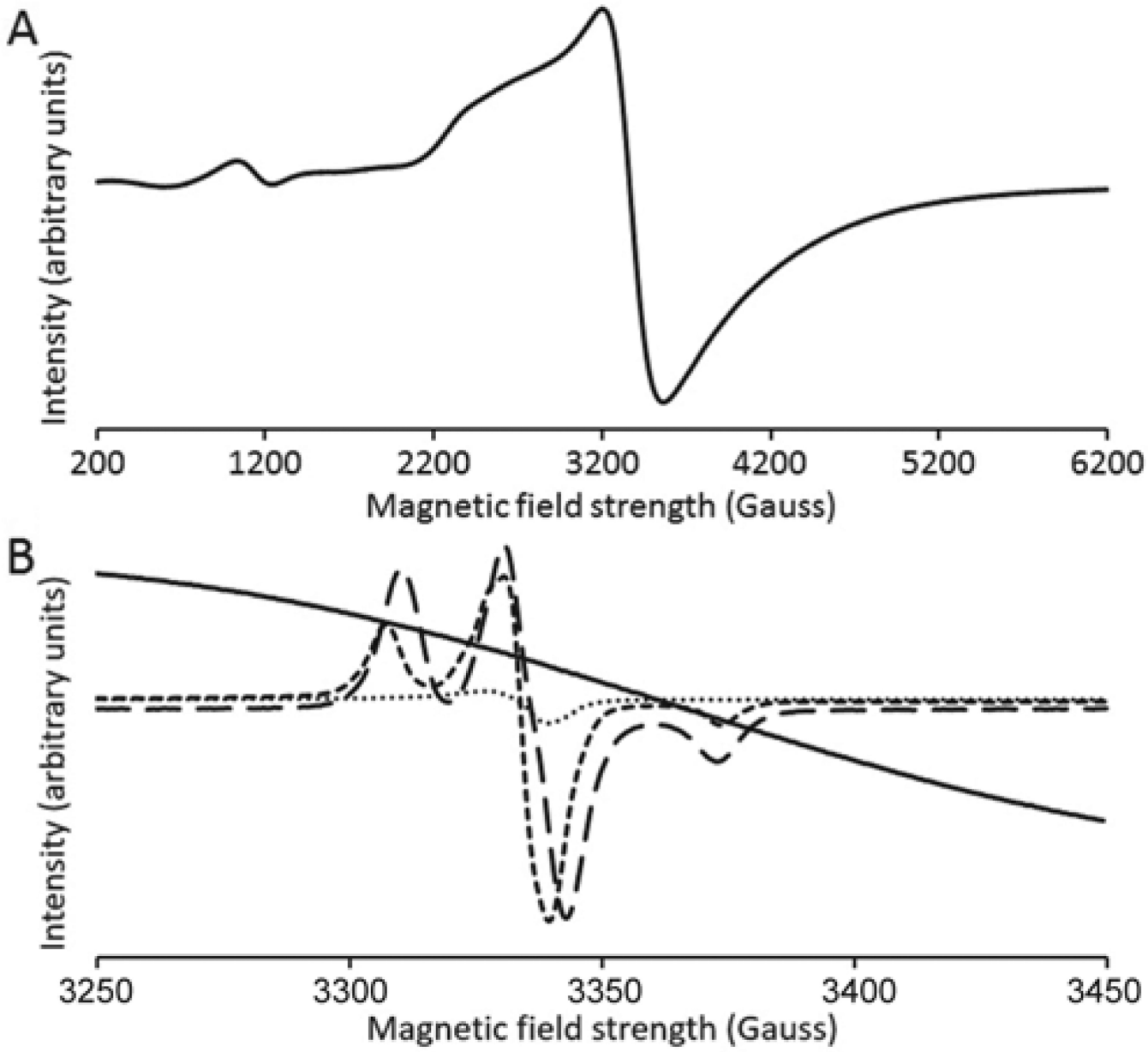

Figure 1.

EPR spectra of (A) $EuCl_2$ + BMPO (wide view) and (B) $EuCl_2$ + BMPO (—), $EuCl_2$ + O_2 + BMPO (— —), KO_2 + BMPO (- -), and KO_2 (· ·) in methanol at 110 K under Ar.

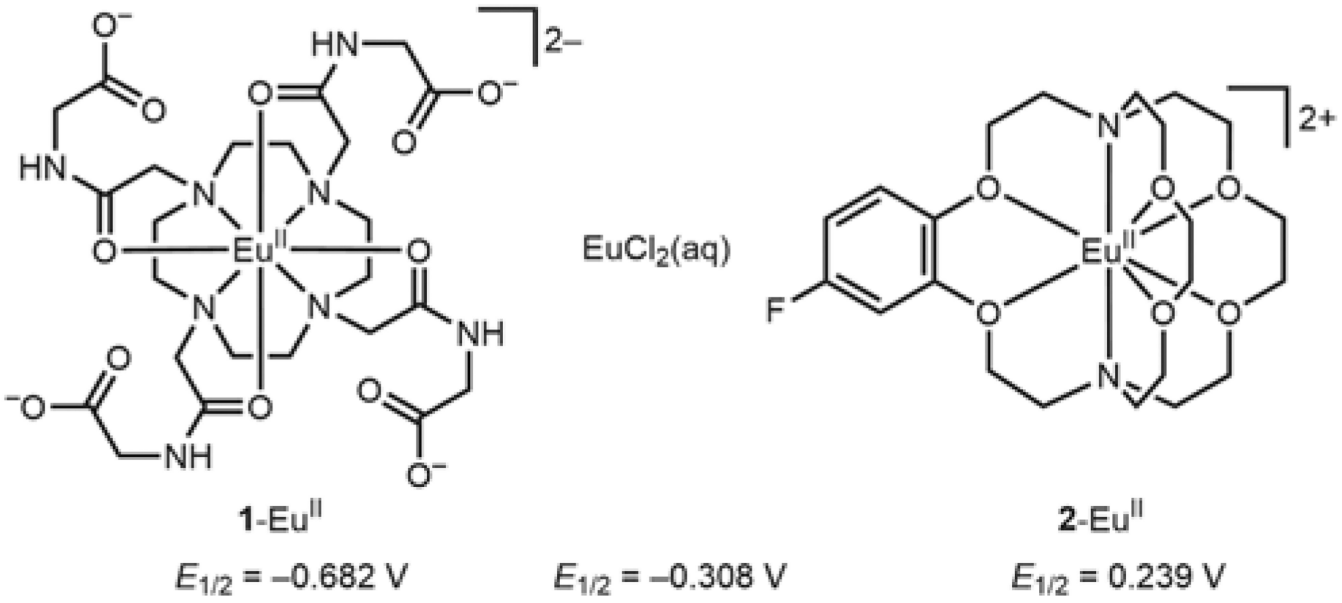

Figure 2.

Macrocyclic tetraglycinate complex **1**-Eu^{II}; the Eu^{II} aqua ion, $EuCl_2(aq)$; and the 4-fluorobenzo-functionalized complex **2**-Eu^{II}. Inner-sphere water and counterions have been omitted for clarity. Reported $E_{1/2}$ values are versus normal hydrogen electrode and are below **1**-Eu^{II},[7], $EuCl_2(aq)$,[17] and **2**-Eu^{II}.[17]

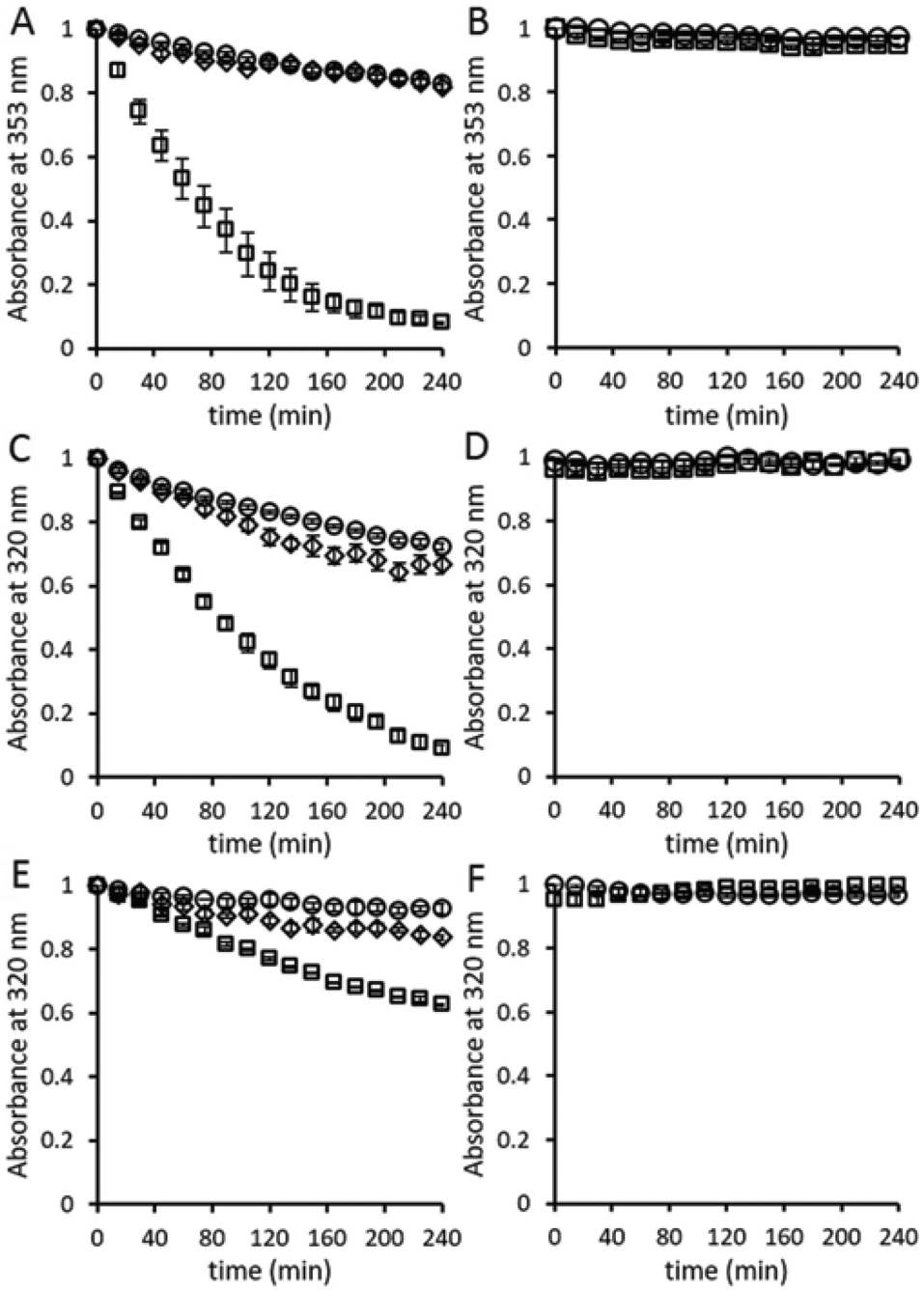

Figure 3.

Normalized absorbance as a function of time at pH 5 (□), 6 (◊), and 7 (○) for **1**-Eu^{II} in the presence of (A) BrO_3^- or (B) GSSG, $EuCl_2$(aq) in the presence of (C) BrO_3^- or (D) GSSG, and **2**-Eu^{II} in the presence of (E) BrO_3^- or (F) GSSG. At the beginning of each reaction, all samples contained Eu^{II} (1.00 mM), acetate (10.0 mM, pH 5), 2-morpholinoethane-1-sulfonate (10.0 mM, pH 6), 3-morpholinopropane-1-sulfonate (MOPS, 10.0 mM, pH 7)

buffer, and oxidant (10.0 mM). Error bars represent the standard error of the mean of three independently prepared samples.

Chemistry. Author manuscript; available in PMC 2018 January 23.

Table 1

Estimated Gibbs free energies (kJ) for redox reactions involving **1**-Eu^{II}, $EuCl_2$(aq), and **2**-Eu^{II} with BrO_3^- or GSSG at pH 5, 6, and 7.

Reaction	BrO_3^- [d] (pH 5)	BrO_3^- [d] (pH 6)	BrO_3^- [d] (pH 7)	GSSG [e] (pH 5)	GSSG [e] (pH 7)
1-Eu^{II} [a]	−1078 [f]	−1043 [f]	−1008	−122 [f]	−99
$EuCl_2$(aq) [b]	−861 [f]	−826 [f]	−792	−50 [f]	−27
2-Eu^{II} [c]	−545 [f]	−510 [f]	−475	56 [f]	79

[a] **1**-Eu^{III} + e^- ⇌ **1**-Eu^{II} (E = −0.682 V);[7]

[b] Eu^{III} + e^- ⇌ Eu^{II} (E = −0.308 V);[17]

[c] **2**-Eu^{III} + e^- ⇌ **2**-Eu^{II} (E = 0.239 V);[17]

[d] BrO_3^- + 6e^- + 6H^+ ⇌ Br^- + 3H_2O (E_{pH5} = 1.18 V, E_{pH6} = 1.12 V, E_{pH7} = 1.06 V);[17]

[e] GSSG + 2e^- + 2H^+ ⇌ 2GSH (E_{pH5} = −0.051 V, E_{pH7} = −0.169 V);[20]

[f] Calculated assuming a 59.1 mV change in reported potential per unit decrease in pH;[19] Estimated Gibbs free energies calculated using $\Delta G = -nFE_{cell}$ where n is the number of electrons, F = 96,458 C mol^{-1}, and $E_{cell} = E_{red} + E_{ox}$. Reduction potentials are listed vs normal hydrogen electrode.

Table 2

k_{ox} ($\times 10^{-3}$ min^{-1}) of **1**-Eu^{II}, $EuCl_2$(aq), and **2**-Eu^{II} with BrO_3^- at pH 5, 6, and 7.[a]

Complex	pH 5	pH 6	pH 7
1-Eu^{II}	12 ± 1	0.7 ± 0.1	0.7 ± 0.1
$EuCl_2$(aq)	9.5 ± 0.6	1.8 ± 0.1	1.3 ± 0.1
2-Eu^{II}	2.0 ± 0.1	0.7 ± 0.1	0.3 ± 0.1

[a]The oxidation of Eu^{II} followed a first-order decay. Accordingly, oxidation rates were calculated using the integrated first-order rate law. Error values represent the standard error of the mean of three independently prepared samples.